

Communication

The Anti-Breast Cancer Activity of Dihydroartemisinin-5-methylisatin Hybrids Tethered via Different Carbon Spacers

Yanfen Yao ¹, Hong Wang ¹, Jing Xu ¹, Feng Gao ² and Wei Cao ^{3,4,*}¹ Shandong Provincial Third Hospital, Shandong University, Jinan 250031, China² State Key Laboratory of Biobased Material and Green Papermaking (LBMP), Qilu University of Technology, Jinan 250353, China³ Department of Nephrology, The First Affiliated Hospital of Shandong First Medical University & Shandong Provincial Qianfoshan Hospital, Shandong Institute of Nephrology, Jinan 250014, China⁴ The First Clinical College, Shandong University of Traditional Chinese Medicine, Jinan 250355, China

* Correspondence: caowei@sdhospital.com.cn

Abstract: Sixteen dihydroartemisinin-5-methylisatin hybrids **6a–c** and **7a–m** tethered via different carbon spacers were assessed for their antiproliferative activity against MCF-7, MDA-MB-231, MCF-7/ADR and MDA-MB-231/ADR breast cancer cell lines as well as cytotoxicity towards MCF-10A cells to investigate the influence of the length of carbon spacers on the activity. The preliminary results illustrated that the length of the carbon spacer was the main parameter which affected the activity, and hybrids tethered via the two-carbon linker showed the highest activity. Amongst the synthesized hybrids, the representative hybrid **7a** (IC₅₀: 15.3–20.1 μM) not only demonstrated profound activity against both drug-sensitive and drug-resistant breast cancer cell lines, but also possessed excellent safety and selectivity profile. Collectively, hybrid **7a** was a promising candidate for the treatment of both drug-sensitive and drug-resistant breast cancers and worthy of further preclinical evaluations.

Keywords: artemisinin; isatin; hybrid molecules; breast cancer; drug resistance



Citation: Yao, Y.; Wang, H.; Xu, J.; Gao, F.; Cao, W. The Anti-Breast Cancer Activity of Dihydroartemisinin-5-methylisatin Hybrids Tethered via Different Carbon Spacers. *Molecules* **2022**, *27*, 7994. <https://doi.org/10.3390/molecules27227994>

Academic Editors: Małgorzata Jelen and Filippo Minutolo

Received: 25 October 2022

Accepted: 16 November 2022

Published: 18 November 2022

Publisher's Note: MDPI stays neutral with regard to jurisdictional claims in published maps and institutional affiliations.



Copyright: © 2022 by the authors. Licensee MDPI, Basel, Switzerland. This article is an open access article distributed under the terms and conditions of the Creative Commons Attribution (CC BY) license (<https://creativecommons.org/licenses/by/4.0/>).

1. Introduction

Breast cancer remains a worldwide public health dilemma and is the most common type of fatal ailment in females around the world [1,2]. Over 2.3 million new cases and 685,000 deaths from breast cancer occurred in 2020, and it is predicted to increase to over 3 million new cases and 1 million deaths by 2040 [3,4]. Diverse therapeutic strategies, inclusive of surgery, chemotherapy, endocrine therapy, targeted therapy, and immunotherapy, have been developed for the treatment of breast cancer. However, drug resistance has become a tremendous obstacle in overcoming recurrence and metastasis and is responsible for most breast cancer fatalities [5,6]. Moreover, current available anti-breast cancer agents could lead to some adverse events such as cardiotoxicity, bronchospasm, sleep disorders, and angioedema [7,8]. Hence, there is a critical need to develop novel anti-breast cancer agents to address drug resistance and side effects.

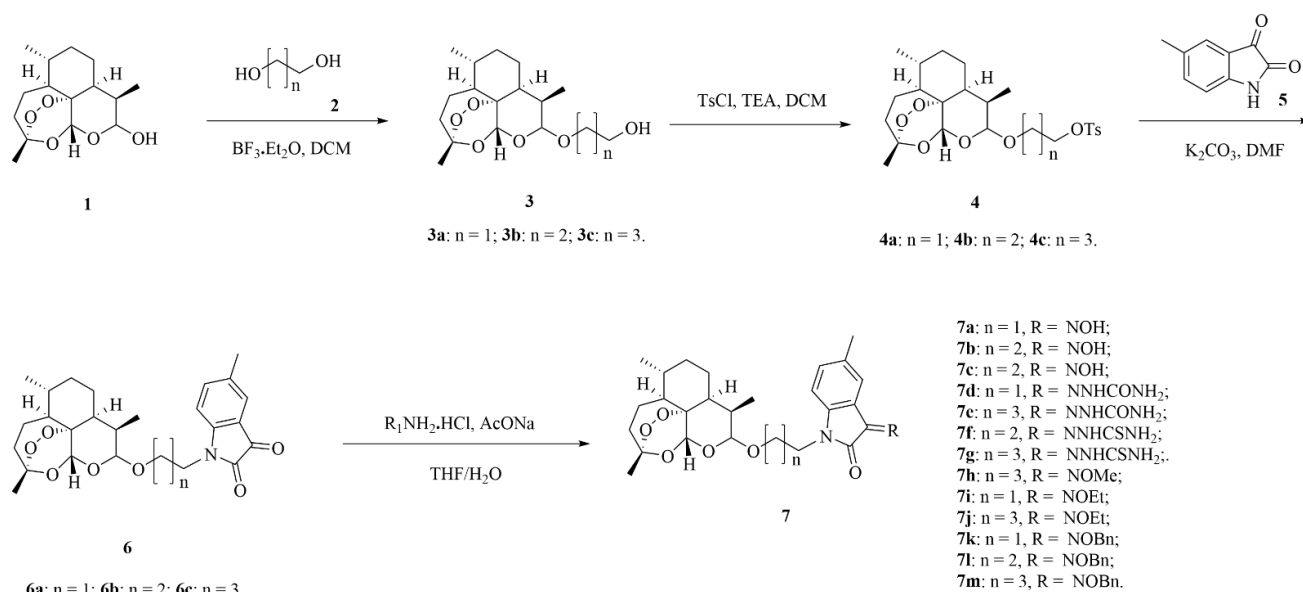
Dihydroartemisinin (DHA), a derivative of artemisinin (ART), demonstrated many advantages compared to ART, including high water solubility, easy absorption, wide distribution, rapid excretion and metabolism, high efficiency, and low toxicity [9,10]. DHA could exert anticancer effects through various mechanisms, such as excessive reactive oxygen species (ROS) production, proliferation inhibition, inducing apoptosis, repression of tumor metastasis and angiogenesis, promotion of immune function, guide of autophagy, and endoplasmic reticulum (ER) stress [11,12]. Accordingly, DHA exhibits profound anticancer activities on a wide range of cancer types including breast cancer both in vitro and in vivo, representing a useful template for the discovery of novel anticancer chemotherapeutics.

Isatin (Indoline-2,3-dione or indole-1*H*-2,3-dione), an endogenous substance, is characterized by a broad range of biological properties such as low toxicity, mutagenicity, and genotoxicity *in vivo* [13,14]. Isatin is a highly “privileged motif” for the target-based design and development of anticancer agents since its derivatives are potential inhibitors of lysine-specific histone demethylase 1 (LSD1), β -carbonic anhydrase, topoisomerase II, tyrosine kinase, proteases, phosphatases, tubulin, and epidermal growth factor receptor (EGFR) [15,16]. Notably, many isatin derivatives have been proved with promising activities against both drug-sensitive and multidrug-resistant breast cancer, and several isatin-based compounds have already been approved for cancer therapy [17,18]. Hence, isatin moiety has also been considered as a useful pharmacophore against breast cancer.

Hybridization of DHA and isatin into one molecule could obtain novel anti-breast cancer candidates with broader spectrum, higher efficiency, lower toxicity, as well as multiple mechanisms of action that could overcome drug resistance [19–22]. DHA-isatin hybrids have the potential in the treatment of breast cancer. As a continuous program to seek for more effective anti-breast cancer candidates, a series of DHA-5-methylisatin hybrids tethered via different carbon spacers were designed, synthesized, and the antiproliferative activities against drug-sensitive MCF-7 and MDA-MB-231 breast cancer cell lines as well as their multidrug-resistant counterparts MCF-7/ADR and MDA-MB-231/ADR were also evaluated in this study.

2. Results and Discussion

The DHA-5-methylisatin hybrids **6a–c** and **7a–m** tethered via different carbon spacers were prepared through the synthetic route depicted in Scheme 1. 2-Hydroxyethyl/3-hydroxypropyl/4-hydroxybutyl were incorporated into C-12 position of DHA skeleton through acetalization of DHA **1** and ethylene glycol/1,3-propylene glycol/1,4-butanediol (**2**) in presence of boron trifluoride diethyl etherate ($\text{BF}_3 \cdot \text{Et}_2\text{O}$). Introduction of *p*-toluenesulfonyl (Ts) to the terminal hydroxyl group of intermediates **3** with triethylamine (TEA) as base yielded intermediates **4**, and then alkylation of 5-methylisatins with tosylates **4** provided desired DHA-5-methylisatin hybrids **6a–c**. Finally, DHA-5-methylisatin hybrids **6a–c** reacted with hydroxyamine/methoxyamine/ethoxyamine/benzyloxyamine hydrochlorides or semicarbazide/thiosemicarbazide by using sodium acetate (AcONa) as base, giving hybrids **7a–m**.



Scheme 1. Synthetic route of DHA-5-methylisatin hybrids **6a–c** and **7a–m**.

The desired DHA-5-methylisatin hybrids **6a–c** and **7a–m** tethered via different carbon spacers were characterized by high resolution mass spectrometry (HRMS), proton nuclear magnetic resonance (^1H NMR), and carbon-13 nuclear magnetic resonance spectroscopy

(^{13}C NMR), and the corresponding analytical spectra were included in the Supplementary Materials. Take hybrid **6a** for an example, the characteristic signals in ^1H NMR as follows: 0.75 (d, 3H), 0.97 (d, 3H), and 1.48 (s, 3H) ppm belongs to $-\text{CH}_3$ at C-3, C-6, and C-9 position of DHA moiety, 4.76 (d, 1H) and 5.19 (s, 1H) belongs to C-10 and C-12 positions, respectively; 3.63–3.67 (m, 1H), 3.87–3.90 (m, 1H), 4.00–4.04 (m, 1H), and 4.14–4.18 (m, 1H) ppm belongs to the $-\text{CH}_2\text{CH}_2-$ linker between DHA and 5-methylisatin; 2.36 (s, 3H) belongs to $-\text{CH}_3$ at C-5 position of isatin moiety, whereas 6.86 (d, 1H), 7.38 (d, 1H) and 7.41 (s, 1H) ppm belongs to isatin moiety. For the HRMS, m/z Calcd for $\text{C}_{26}\text{H}_{33}\text{NO}_7\text{Na}$ $[\text{M} + \text{Na}]^+$: 494.2149; Found: 494.2147. Based on the above analysis, the structure of hybrid **6a** was correct.

The antiproliferative activity and cytotoxicity of DHA-5-methylisatin hybrids **6a–c** and **7a–m** against MCF-7, MDA-MB-231, MCF-7/ADR, and MDA-MB-231/ADR (Purchased from Procell) breast cancer cell lines as well as MCF-10A were assessed by 3-(4,5-dimethylthiazol-2-yl)-2,5-diphenyltetrazolium bromide (MTT) assay. The antiproliferative activity and cytotoxicity were expressed in terms of half maximal inhibitory concentration (IC_{50}) values in Tables 1 and 2, respectively.

As can be seen from Table 1, most of the synthesized hybrids (IC_{50} : 15.3–99.9 μM) were active against MCF-7, MDA-MB-231, MCF-7/ADR, and MDA-MB-231/ADR breast cancer cell lines. The SARs illustrated that the carbon spacers between DHA and isatin moieties were the main parameter influenced the activity, and the relative contribution order was two-carbon > four-carbon > three-carbon. Hydrogen bond donors at C-3 position of isatin moiety could enhance the activity, and the relative contribution order was $\text{NOH} > \text{NNHCSNH}_2 > \text{NNHCONH}_2$. Additionally, alkyloxime at C-3 position of isatin moiety could improve the activity to some extent, while benzoxime decreased the activity.

Table 1. The antiproliferative activity of DHA-5-methylisatin hybrids **6a–c** and **7a–m**.

| Hybrid | Antiproliferative Activity (IC_{50} : μM) | | | |
|-------------------------|---|------------|-----------|----------------|
| | MCF-7 | MDA-MB-231 | MCF-7/ADR | MDA-MB-231/ADR |
| 6a | 31.7 | 29.1 | 25.3 | 26.9 |
| 6b | >100 | >100 | 87.4 | >100 |
| 6c | 59.7 | 42.3 | 49.9 | 44.5 |
| 7a | 19.4 | 15.3 | 20.1 | 18.8 |
| 7b | 30.3 | 42.6 | 28.7 | 36.4 |
| 7c | 22.1 | 26.7 | 23.4 | 28.5 |
| 7d | 27.2 | 19.7 | 33.3 | 21.6 |
| 7e | 39.0 | 31.2 | 42.1 | 34.5 |
| 7r | 46.7 | 48.2 | 36.4 | 51.1 |
| 7g | 28.9 | 35.1 | 30.3 | 40.6 |
| 7h | 85.2 | 73.9 | 77.5 | 80.3 |
| 7i | 69.3 | 70.4 | 61.8 | 72.7 |
| 7j | 99.9 | 86.8 | 90.4 | 97.1 |
| 7k | >100 | >100 | >100 | >100 |
| 7l | >100 | >100 | >100 | >100 |
| 7m | >100 | >100 | >100 | >100 |
| ART ^a | 87.6 | 72.4 | >100 | >100 |
| DHA ^b | 73.2 | 69.6 | 79.1 | 82.8 |
| ADR ^c | 18.9 | 4.46 | >100 | >100 |

^a ART: Artemisinin; ^b DHA: Dihydroartemisinin; ^c ADR: Adriamycin.

Table 2. The cytotoxicity, selectivity index and resistance index values of DHA-5-methylisatin hybrids 6a–c and 7a–m.

| Hybrid | Cytotoxicity (IC ₅₀ : μM) | | SI ^a | | RI ^d | |
|--------|--------------------------------------|------------------|------------------|------------------|------------------|--|
| | MCF-10A | SI1 ^b | SI2 ^c | RI1 ^e | RI2 ^f | |
| 6a | >100 | >3.15 | >3.43 | 0.80 | 0.92 | |
| 6b | >100 | – | – | <0.87 | – | |
| 6c | >100 | >1.67 | >2.36 | 0.83 | 1.05 | |
| 7a | >100 | >5.15 | >6.53 | 1.03 | 1.23 | |
| 7b | >100 | >3.30 | >2.34 | 0.95 | 0.85 | |
| 7c | >100 | >4.52 | >3.83 | 1.06 | 1.07 | |
| 7d | >100 | >3.67 | >5.07 | 1.22 | 1.10 | |
| 7e | >100 | >2.56 | >3.20 | 1.08 | 1.11 | |
| 7f | >100 | >2.14 | >2.07 | 0.78 | 1.06 | |
| 7g | >100 | >3.46 | >2.84 | 1.05 | 1.16 | |
| 7h | >100 | >1.17 | >1.35 | 0.91 | 1.09 | |
| 7i | >100 | >1.44 | >1.42 | 0.89 | 1.03 | |
| 7j | >100 | >1.00 | >1.15 | 0.90 | 1.12 | |
| 7k | >100 | – | – | – | – | |
| 7l | >100 | – | – | – | – | |
| 7m | >100 | – | – | – | – | |
| ART | >100 | >1.14 | >1.38 | >1.14 | >1.38 | |
| DHA | >100 | >1.36 | >1.43 | 1.08 | 1.19 | |
| ADR | 68.8 | 3.64 | 14.76 | >5.29 | >22.42 | |

^a SI: Selectivity index, IC₅₀(normal cell)/IC₅₀(cancer cell); ^b SI1: IC₅₀(MCF-10A)/IC₅₀(MCF-7); ^c SI2: IC₅₀(MCF-10A)/IC₅₀(MDA-MB-231); ^d RI: Resistance index, IC₅₀(drug-resistant cancer cell)/IC₅₀(drug-sensitive cancer cell); ^e RI1: IC₅₀(MCF-7/ADR)/IC₅₀(MCF-7); ^f RI2: IC₅₀(MDA-MB-231/ADR)/IC₅₀(MDA-MB-231).

From Table 2, all hybrids (IC₅₀: >100 μM) displayed non-cytotoxicity towards normal MCF-10A breast cells, while the reference adriamycin (IC₅₀: 68.8 μM) showed moderate cytotoxicity. The selectivity index (SI: IC₅₀(MCF-10A)/IC₅₀(MCF-7) and IC₅₀(MCF-10A)/IC₅₀(MDA-MB-231)) values of seven hybrids were >2.07, and the resistance index (RI: IC₅₀(MCF-7/ADR)/IC₅₀(MCF-7) and IC₅₀(MDA-MB-231/ADR)/IC₅₀(MDA-MB-231)) values were in a range of 0.78 to 1.22, demonstrating that the synthesized hybrids had no cross resistance with adriamycin.

Hybrid 7a (IC₅₀: 15.3–20.1 μM) was found to be most active against MCF-7, MDA-MB-231, MCF-7/ADR, and MDA-MB-231/ADR breast cancer cell lines. The activity was comparable to that of adriamycin (IC₅₀: 18.9 μM) against MCF-7 cells, but >4.97 times superior to adriamycin (IC₅₀: >100 μM) against MCF-7/ADR and MDA-MB-231/ADR cancer cell lines. The RI values of hybrid 7a were 1.03 and 1.23 respectively, proving its potential to overcome drug resistance. Moreover, hybrid 7a (IC₅₀: >100 μM) was non-toxic towards normal MCF-10A breast cells, and the SI values were >5.15 and >6.53, revealing its excellent safety and selectivity profiles. It seems that the hydrogen bond donors especially NOH at C-3 position of isatin moiety showed higher SI values.

3. Experimental Section

3.1. Chemistry

3.1.1. General

¹H NMR and ¹³C spectra were determined on a Mercury-400 spectrometer (Varian, Palo Alto, CA, USA) in DMSO-*d*₆ or CDCl₃ using tetramethylsilane (TMS) as an internal

standard. Electrospray ionization (ESI) mass spectra and high-resolution mass spectra (HRMS) were obtained on a Q-Tap mass spectrometer (MDSSCIEX, Concord, CA, USA) and AccuTOF CS JMS-T100CS mass spectrometer (JEOL, Tokyo, Japan), respectively. Unless otherwise noted, the reagents were obtained from commercial supplier and used without further purification.

3.1.2. General Procedure for the Synthesis

To the mixture of dihydroartemisinin 1 (80 mmol) and ethylene glycol/1,3-propylene glycol/1,4-butanediol 2 (100 mmol) in DCM (500 mL), boron trifluoride diethyl etherate (20 mL) was added at 0 °C. The mixture was stirred at 25 °C for 12 h, and then quenched by sat. Na₂CO₃ (500 mL) slowly. The organic layer was washed with H₂O (300 mL), dried over anhydrous Na₂SO₄, filtrated, and concentrated under reduced pressure. The residue was purified by silica gel chromatography eluted with PE to PE:EA = 1:1 to give intermediates **3a–c**. To the mixture of DHA intermediates **3a–c** (50 mmol) and triethylamine (100 mmol) in DCM (400 mL), *p*-toluenesulfonyl chloride (60 mmol) in was added. The mixture was stirred at room temperature for 5 h, and then H₂O (300 mL) was added. The organic layer was dried over anhydrous Na₂SO₄, filtrated, and concentrated in vacuo to give crude tosylates **4a–c** which were used directly in the next step. The mixture of 5-methylisatin 5 (12 mmol) and potassium carbonate (K₂CO₃, 20 mmol) in DMF (50 mL) was stirred at room temperature for 30 min, and then crude tosylates **4a–c** (10 mmol) was added. The mixture was stirred overnight at room temperature, and then filtered. The filtrate was concentrated under reduced pressure to give the residue which was purified by silica gel chromatography eluted with PE to PE:EA = 1:1 to provide DHA-isatin hybrids **6a–c**. To a solution of hybrids **6a–c** (1 mmol) and hydroxyamine/methoxyamine/ethoxyamine/benzyloxyamine hydrochlorides or semicarbazide/thiosemicarbazide in a mixture of THF (10 mL) and H₂O (10 mL), sodium acetate (2.0 mmol) was added. The mixture was stirred at 60 °C for 12 h, and after cooling to room temperature, the mixture was extracted with DCM (20 mL × 3). The combined organic layers were washed with H₂O (30 mL), dried over anhydrous Na₂SO₄, filtrated, and concentrated under reduced pressure. The residue was purified by silica gel chromatography eluted with PE to PE:EA = 1:1 to give C-3 modified hybrids **7a–m**.

5-Methyl-1-(2-(((3R,5aS,6R,8aS,9R,12R,12aR)-3,6,9-trimethyldecahydro-12H-3,12-epoxy[1,2]dioxepino[4,3-*i*]isochromen-10-yl)oxy)ethyl)indoline-2,3-dione (**6a**)

Red solid. ¹H NMR (600 Hz, CDCl₃) 0.75–0.91 (m, 7H), 1.03–1.05 (m, 1H), 1.15–1.19 (m, 1H), 1.36–1.43 (m, 5H), 1.46–1.57 (m, 3H), 1.81–1.86 (m, 1H), 1.98–2.02 (m, 1H), 2.30–2.35 (m, 4H), 2.55–2.58 (m, 1H), 3.63–3.67 (m, 1H), 3.87–3.90 (m, 1H), 4.00–4.04 (m, 1H), 4.14–4.18 (m, 1H), 4.76 (d, *J* = 2.0 Hz, 1H), 5.19 (s, 1H), 6.86 (d, *J* = 4.0 Hz, 1H), 7.38 (d, *J* = 4.0 Hz, 1H), 7.41 (s, 1H). ¹³C NMR (150 Hz, CDCl₃) 183.46, 158.46, 138.52, 133.52, 125.65, 117.58, 110.49, 104.14, 102.42, 87.80, 80.85, 64.60, 60.41, 52.33, 44.10, 40.03, 37.39, 36.32, 34.40, 30.66, 26.08, 24.62, 24.46, 20.64, 20.24, 12.81. HRMS-ESI: *m/z* Calcd for C₂₆H₃₃NO₇Na [M + Na]⁺: 494.2149; Found: 494.2147.

5-Methyl-1-(3-(((3R,5aS,6R,8aS,9R,12R,12aR)-3,6,9-trimethyldecahydro-12H-3,12-epoxy[1,2]dioxepino[4,3-*i*]isochromen-10-yl)oxy)propyl)indoline-2,3-dione (**6b**)

Brown solid. ¹H NMR (600 Hz, DMSO-*d*₆) δ 0.92–1.02 (m, 7H), 1.25–1.37 (m, 3H), 1.41–1.59 (m, 4H), 1.63–1.70 (m, 1H), 1.77–1.82 (m, 1H), 1.87–1.99 (m, 3H), 2.02–2.06 (m, 2H), 2.34 (s, 3H, CH₃), 2.36–2.44 (m, 1H), 2.66–2.68 (m, 1H), 3.46–3.51 (m, 1H), 3.66–4.14 (m, 3H), 4.80 (d, *J* = 2.0 Hz, 1H), 5.54 (s, 1H), 6.82 (d, *J* = 4.0 Hz, 1H), 7.36–7.42 (m, 2H). ¹³C NMR (150 Hz, DMSO-*d*₆) 183.98, 183.74, 158.48, 158.25, 148.79, 138.99, 138.80, 138.63, 133.53, 133.38, 125.92, 125.85, 125.63, 117.68, 117.57, 110.49, 110.00, 109.82, 104.29, 104.16, 102.14, 100.32, 91.23, 87.95, 81.03, 80.41, 66.06, 65.51, 58.86, 52.55, 51.66, 45.37, 44.38, 37.44, 36.40,

27.75, 26.16, 24.66, 24.57, 20.66, 20.65, 20.37, 14.20, 13.09, 12.72. HRMS-ESI: m/z Calcd for $C_{27}H_{35}NO_7Na$ $[M + Na]^+$: 508.2306; Found: 508.2277.

5-Methyl-1-(4-(((3R,5aS,6R,8aS,9R,12R,12aR)-3,6,9-trimethyldecahydro-12H-3,12-epoxy[1,2]dioxepino[4,3-i]isochromen-10-yl)oxy)butyl)indoline-2,3-dione (**6c**)

Yellow solid. 1H NMR (600 Hz, $CDCl_3$) 0.85–0.96 (m, 7H), 1.22–1.32 (m, 3H), 1.40–1.53 (m, 5H), 1.68–1.79 (m, 7H), 1.85–1.89 (m, 1H), 2.01–2.05 (m, 1H), 2.33–2.40 (m, 4H), 2.60–2.63 (m, 1H), 3.39–3.49 (m, 1H), 3.71–4.02 (m, 3H), 4.76 (d, $J = 2.0$ Hz, 1H), 5.35 (s, 1H), 6.78 (d, $J = 8.0$ Hz, 1H), 7.37–7.42 (m, 2H). ^{13}C NMR (150 Hz, $CDCl_3$) 183.81, 158.27, 148.76, 138.93, 138.62, 133.50, 125.86, 117.69, 110.36, 109.88, 104.26, 104.12, 102.13, 100.02, 91.22, 87.92, 81.07, 67.77, 52.55, 51.68, 44.39, 40.05, 37.45, 36.43, 34.59, 30.88, 27.23, 26.18, 24.64, 24.51, 24.31, 20.66, 20.36, 13.04, 12.65. HRMS-ESI: m/z Calcd for $C_{28}H_{37}NO_7Na$ $[M + Na]^+$: 522.2462; Found: 522.2461.

3-(Hydroxyimino)-5-methyl-1-(2-(((3R,5aS,6R,8aS,9R,12R,12aR)-3,6,9-trimethyldecahydro-12H-3,12-epoxy[1,2]dioxepino[4,3-i]isochromen-10-yl)oxy)ethyl)indolin-2-one (**7a**)

Yellow solid. 1H NMR (600 Hz, $CDCl_3$) 0.74–0.88 (m, 7H), 0.95–0.98 (m, 1H), 1.10–1.15 (m, 1H), 1.33–1.36 (m, 2H), 1.40 (s, 3H), 1.43–1.46 (m, 2H), 1.53–1.56 (m, 1H), 1.77–1.81 (m, 1H), 1.96–1.99 (m, 1H), 2.25–2.31 (m, 1H), 2.34 (s, 3H), 2.53–2.56 (m, 1H), 3.61–3.64 (m, 1H), 3.86–3.90 (m, 1H), 4.08–4.12 (m, 1H), 4.19–4.23 (m, 1H), 4.76 (d, $J = 2.0$ Hz, 1H), 5.12 (s, 1H), 6.82 (d, $J = 4.0$ Hz, 1H), 7.18 (d, $J = 4.0$ Hz, 1H), 7.95 (s, 1H), 10.98 (brs, 1H). ^{13}C NMR (150 Hz, $CDCl_3$) 144.51, 141.42, 132.72, 132.45, 128.80, 108.98, 104.09, 102.19, 87.77, 80.92, 64.47, 52.35, 44.16, 39.74, 37.50, 37.27, 36.35, 34.44, 30.70, 26.10, 24.59, 24.43, 20.96, 20.25, 12.80. HRMS-ESI: m/z Calcd for $C_{26}H_{34}N_2O_8Na$ $[M + Na]^+$: 509.2258; Found: 509.2266.

3-(Hydroxyimino)-5-methyl-1-(3-(((3R,5aS,6R,8aS,9R,12R,12aR)-3,6,9-trimethyldecahydro-12H-3,12-epoxy[1,2]dioxepino[4,3-i]isochromen-10-yl)oxy)propyl)indolin-2-one (**7b**)

Yellow solid. 1H NMR (600 Hz, $DMSO-d_6$) δ 0.84–0.99 (m, 7H), 1.24–1.37 (m, 3H), 1.43–1.59 (m, 5H), 1.64–1.68 (m, 1H), 1.78–1.82 (m, 1H), 1.87–1.98 (m, 2H), 2.01–2.06 (m, 2H), 2.34 (s, 3H, CH₃), 2.36–2.44 (m, 1H), 2.64–2.68 (m, 1H), 3.43–3.52 (m, 1H), 3.70–4.14 (m, 3H), 4.81 (d, $J = 2.0$ Hz, 1H), 5.45 (s, 1H), 6.76 (d, $J = 4.0$ Hz, 1H), 7.16 (d, $J = 4.0$ Hz, 1H), 7.95 (s, 1H). ^{13}C NMR (150 Hz, $DMSO-d_6$) 164.25, 144.55, 141.38, 134.99, 132.77, 132.63, 132.49, 128.96, 128.79, 115.78, 108.84, 108.47, 108.30, 104.32, 104.19, 102.13, 100.30, 91.24, 89.70, 97.97, 81.11, 80.43, 66.29, 65.66, 60.45, 58.65, 52.57, 51.67, 51.44, 45.39, 44.44, 37.48, 37.41, 36.42, 34.66, 30.90, 28.01, 26.16, 24.70, 24.66, 24.57, 20.97, 20.39, 20.29, 13.09, 12.73. HRMS-ESI: m/z Calcd for $C_{27}H_{36}N_2O_7Na$ $[M + Na]^+$: 523.2415; Found: 523.2394.

3-(Hydroxyimino)-5-methyl-1-(4-(((3R,5aS,6R,8aS,9R,12R,12aR)-3,6,9-trimethyldecahydro-12H-3,12-epoxy[1,2]dioxepino[4,3-i]isochromen-10-yl)oxy)butyl)indolin-2-one (**7c**)

Yellow solid. 1H NMR (600 Hz, $CDCl_3$) 0.84–0.99 (m, 7H), 1.21–1.30 (m, 3H), 1.42–1.53 (m, 5H), 1.58–1.82 (m, 6H), 1.85–1.88 (m, 1H), 2.01–2.05 (m, 1H), 2.31–2.38 (m, 4H), 2.60–2.62 (m, 1H), 3.38–3.41 (m, 1H), 3.73–3.89 (m, 3H), 4.76 (d, $J = 2.0$ Hz, 1H), 5.36 (s, 1H), 6.14 (d, $J = 4.0$ Hz, 1H), 7.18 (d, $J = 4.0$ Hz, 1H), 7.93 (d, $J = 4.0$ Hz, 1H), 10.84 (brs, 1H). ^{13}C NMR (150 Hz, $CDCl_3$) 132.73, 108.39, 104.12, 102.08, 100.05, 91.22, 87.92, 81.11, 67.84, 52.57, 44.42, 39.80, 37.43, 36.43, 34.58, 30.90, 27.20, 26.18, 24.64, 24.50, 24.11, 20.97, 20.36, 20.28, 13.04, 12.64. HRMS-ESI: m/z Calcd for $C_{28}H_{38}N_2O_8Na$ $[M + Na]^+$: 537.2571; Found: 537.2568.

2-(5-Methyl-2-oxo-1-(2-(((3R,5aS,6R,8aS,9R,12R,12aR)-3,6,9-trimethyldecahydro-12H-3,12-epoxy[1,2]dioxepino[4,3-i]isochromen-10-yl)oxy)ethyl)indolin-3-ylidene)hydrazine-1-carboxamide (**7d**)

Yellow solid. ^1H NMR (600 Hz, CDCl_3) 0.75–0.91 (m, 7H), 1.04–1.06 (m, 1H), 1.14–1.18 (m, 1H), 1.36–1.40 (m, 5H), 1.46–1.51 (m, 2H), 1.56–1.59 (m, 1H), 1.81–1.85 (m, 1H), 1.98–2.01 (m, 1H), 2.30–2.35 (m, 4H), 2.55–2.58 (m, 1H), 3.63–3.67 (m, 1H), 3.86–3.90 (m, 1H), 4.00–4.03 (m, 1H), 4.14–4.18 (m, 1H), 4.76 (d, $J = 2.0$ Hz, 1H), 5.19 (s, 1H), 6.86 (d, $J = 4.0$ Hz, 1H), 7.38 (d, $J = 4.0$ Hz, 1H), 7.41 (s, 1H). ^{13}C NMR (150 Hz, CDCl_3) 183.47, 158.47, 148.82, 138.52, 133.52, 125.65, 117.58, 110.49, 104.15, 102.42, 87.81, 80.85, 64.61, 52.34, 44.10, 40.04, 37.39, 36.32, 34.40, 30.66, 26.09, 24.62, 24.46, 20.65, 20.25, 12.82.

2-(5-Methyl-2-oxo-1-(4-(((3R,5aS,6R,8aS,9R,12R,12aR)-3,6,9-trimethyldecahydro-12H-3,12-epoxy[1,2]dioxepino[4,3-i]isochromen-10-yl)oxy)butyl)indolin-3-ylidene)hydrazine-1-carboxamide (**7e**)

Yellow solid. ^1H NMR (600 Hz, CD_3OD) 0.72–0.87 (m, 7H), 1.06–1.14 (m, 2H), 1.22–1.32 (m, 5H), 1.39–1.48 (m, 1H), 1.55–1.77 (m, 7H), 1.90–1.94 (m, 1H), 2.16–2.25 (m, 4H), 2.39–2.42 (m, 1H), 3.36–3.86 (m, 4H), 4.60 (d, $J = 2.0$ Hz, 1H), 5.23 (s, 1H), 6.92 (d, $J = 4.0$ Hz, 1H), 7.30–7.39 (m, 2H). ^{13}C NMR (150 Hz, $\text{DMSO}-d_6$) 187.55, 162.82, 152.73, 142.47, 142.33, 137.44, 128.74, 121.78, 114.21, 107.96, 106.25, 104.00, 95.17, 91.78, 84.71, 84.22, 71.85, 56.47, 48.36, 43.48, 41.17, 39.90, 38.28, 34.92, 28.56, 28.27, 28.24, 28.19, 23.30, 23.14, 15.90, 15.52.

2-(5-Methyl-2-oxo-1-(3-(((3R,5aS,6R,8aS,9R,12R,12aR)-3,6,9-trimethyldecahydro-12H-3,12-epoxy[1,2]dioxepino[4,3-i]isochromen-10-yl)oxy)propyl)indolin-3-ylidene)hydrazine-1-carbothioamide (**7f**)

Yellow solid. ^1H NMR (600 Hz, CD_3OD) 0.93–1.02 (m, 7H), 1.23–1.34 (m, 2H), 1.40–1.50 (m, 4H), 1.52–1.59 (m, 1H), 1.65–1.73 (m, 2H), 1.77–1.91 (m, 2H), 1.94–2.06 (m, 3H), 2.34–2.39 (m, 4H), 2.64–2.66 (m, 3H), 3.42–3.49 (m, 1H), 3.73–4.05 (m, 3H), 4.80 (d, $J = 2.0$ Hz, 1H), 5.48 (s, 1H), 6.62 (brs, 1H), 6.80 (d, $J = 4.0$ Hz, 1H), 7.18 (d, $J = 4.0$ Hz, 1H), 7.40 (s, 1H), 7.52 (brs, 1H), 12.88 (s, 1H). ^{13}C NMR (150 Hz, $\text{DMSO}-d_6$) 180.01, 161.11, 141.13, 132.91, 132.00, 121.57, 119.44, 109.12, 104.17, 102.17, 87.96, 81.12, 65.34, 52.66, 44.42, 37.35, 37.22, 36.43, 30.90, 27.90, 26.18, 24.69, 24.54, 21.02, 20.47, 13.09, 12.71. HRMS-ESI: m/z Calcd for $\text{C}_{28}\text{H}_{38}\text{N}_4\text{O}_6\text{SNa}$ [$\text{M} + \text{Na}$] $^+$: 581.2404; Found: 581.2377. HRMS-ESI: m/z Calcd for $\text{C}_{28}\text{H}_{37}\text{N}_4\text{O}_6\text{S}$ [$\text{M} - \text{H}$] $^+$: 577.2439; Found: 577.2428.

2-(5-Methyl-2-oxo-1-(4-(((3R,5aS,6R,8aS,9R,12R,12aR)-3,6,9-trimethyldecahydro-12H-3,12-epoxy[1,2]dioxepino[4,3-i]isochromen-10-yl)oxy)butyl)indolin-3-ylidene)hydrazine-1-carbothioamide (**7g**)

Yellow solid. ^1H NMR (600 Hz, $\text{DMSO}-d_6$) 0.76–0.89 (m, 7H), 1.08–1.18 (m, 2H), 1.23–1.34 (m, 5H), 1.40–1.49 (m, 1H), 1.54–1.70 (m, 6H), 1.72–1.77 (m, 1H), 1.95–1.98 (m, 1H), 2.12–2.17 (m, 1H), 2.34–2.36 (m, 1H), 3.36–3.44 (m, 1H), 3.67–3.78 (m, 3H), 4.65 (d, $J = 2.0$ Hz, 1H), 5.21 (s, 1H), 7.06 (d, $J = 4.0$ Hz, 1H), 7.22 (d, $J = 4.0$ Hz, 1H), 7.55 (s, 1H), 8.69 (s, 1H), 9.03 (s, 1H), 12.40 (s, 1H). ^{13}C NMR (150 Hz, $\text{DMSO}-d_6$) 183.93, 165.98, 145.97, 137.12, 126.63, 126.41, 126.49, 124.69, 114.93, 108.49, 106.32, 92.15, 85.64, 72.50, 57.27, 49.03, 41.91, 35.73, 30.78, 25.83, 25.44, 17.98. HRMS-ESI: m/z Calcd for $\text{C}_{29}\text{H}_{40}\text{N}_4\text{O}_6\text{SNa}$ [$\text{M} + \text{Na}$] $^+$: 595.2561; Found: 595.2525.

3-(Methoxyimino)-1-(4-(((3R,5aS,6R,8aS,9R,12R,12aR)-3,6,9-trimethyldecahydro-12H-3,12-epoxy[1,2]dioxepino[4,3-i]isochromen-10-yl)oxy)butyl)indolin-2-one (**7h**)

Yellow solid. ^1H NMR (600 Hz, CDCl_3) 0.85–0.96 (m, 7H), 1.20–1.30 (m, 2H), 1.41–1.52 (m, 5H), 1.57–1.78 (m, 7H), 1.84–1.89 (m, 1H), 2.01–2.04 (m, 1H), 2.33–2.38 (m, 1H), 2.59–2.63 (m, 1H), 3.37–3.41 (m, 1H), 3.73–3.82 (m, 2H), 3.85–3.88 (m, 1H), 4.30 (s, 3H), 4.76 (d,

$J = 2.0$ Hz, 1H), 5.35 (s, 1H), 6.82 (d, $J = 8.0$ Hz, 1H), 7.06 (t, $J = 8.0$ Hz, 1H), 7.38 (t, $J = 4.0$ Hz, 1H), 7.96 (d, $J = 4.0$ Hz, 1H). ^{13}C NMR (150 Hz, CDCl_3) 163.47, 143.85, 143.61, 132.38, 128.04, 122.82, 115.88, 108.58, 104.08, 102.04, 87.90, 81.10, 67.80, 64.75, 52.57, 44.42, 39.73, 37.43, 36.44, 34.59, 30.89, 27.17, 26.20, 24.65, 24.49, 24.47, 20.35, 13.03. HRMS-ESI: m/z Calcd for $\text{C}_{28}\text{H}_{38}\text{N}_2\text{O}_7\text{Na}$ $[\text{M} + \text{Na}]^+$: 537.2555; Found: 537.2571.

3-(Ethoxyimino)-5-methyl-1-(2-(((3R,5aS,6R,8aS,9R,12R,12aR)-3,6,9-trimethyldecahydro-12H-3,12-epoxy[1,2]dioxepino[4,3-i]isochromen-10-yl)oxy)ethyl)indolin-2-one (7i)

Yellow solid. ^1H NMR (600 Hz, CDCl_3) 0.73–0.90 (m, 7H), 0.92–1.00 (m, 1H), 1.33–1.36 (m, 2H), 1.40 (s, 3H), 1.43–1.47 (m, 5H), 1.54–1.57 (m, 1H), 1.79–1.82 (m, 1H), 1.96–2.02 (m, 1H), 2.29–2.32 (m, 1H), 2.34 (s, 3H), 2.52–2.55 (m, 1H), 3.59–3.62 (m, 1H), 3.83–3.87 (m, 1H), 4.07–4.12 (m, 1H), 4.16–4.20 (m, 1H), 4.56 (q, $J = 8.0$ Hz, 1H), 4.74 (d, $J = 4.0$ Hz, 1H), 5.12 (s, 1H), 6.80 (d, $J = 8.0$ Hz, 1H), 7.16 (d, $J = 8.0$ Hz, 1H), 7.78 (s, 1H). ^{13}C NMR (150 Hz, CDCl_3) 163.79, 143.53, 141.54, 132.37, 132.30, 128.38, 115.85, 108.88, 104.03, 102.18, 87.73, 80.90, 72.94, 64.52, 52.36, 44.18, 39.59, 37.26, 36.36, 34.47, 30.71, 26.11, 24.60, 24.42, 21.00, 20.25, 14.80, 12.80. HRMS-ESI: m/z Calcd for $\text{C}_{27}\text{H}_{39}\text{N}_2\text{O}_7$ $[\text{M} + \text{H}_3\text{O}]^+$: 519.2701; Found: 519.2194.

3-(Ethoxyimino)-5-methoxy-1-(4-(((3R,5aS,6R,8aS,9R,12R,12aR)-3,6,9-trimethyldecahydro-12H-3,12-epoxy[1,2]dioxepino[4,3-i]isochromen-10-yl)oxy)butyl)indolin-2-one (7j)

Yellow solid. ^1H NMR (600 Hz, CDCl_3) 0.84–0.96 (m, 7H), 1.20–1.30 (m, 2H), 1.41–1.51 (m, 7H), 1.58–1.66 (m, 4H), 1.68–1.77 (m, 4H), 1.85–1.88 (m, 1H), 2.01–2.04 (m, 1H), 2.33–2.38 (m, 4H), 2.59–2.62 (m, 1H), 3.36–3.40 (m, 1H), 3.71–3.78 (m, 2H), 3.84–3.88 (m, 1H), 4.56 (q, $J = 4.0$ Hz, 1H), 4.76 (d, $J = 4.0$ Hz, 1H), 5.35 (s, 1H), 6.72 (d, $J = 4.0$ Hz, 1H), 7.17 (d, $J = 4.0$ Hz, 1H), 7.80 (s, 1H). ^{13}C NMR (150 Hz, CDCl_3) 163.63, 143.64, 141.52, 132.48, 132.30, 128.56, 108.28, 104.04, 102.04, 87.90, 81.11, 72.94, 67.85, 52.58, 44.43, 39.70, 37.43, 36.45, 34.59, 30.91, 27.17, 26.21, 24.65, 24.50, 21.01, 20.36, 14.80, 13.04. HRMS-ESI: m/z Calcd for $\text{C}_{30}\text{H}_{42}\text{N}_2\text{O}_7\text{Na}$ $[\text{M} + \text{Na}]^+$: 565.2884; Found: 565.2850.

3-((Benzyloxy)imino)-5-methyl-1-(2-(((3R,5aS,6R,8aS,9R,12R,12aR)-3,6,9-trimethyldecahydro-12H-3,12-epoxy[1,2]dioxepino[4,3-i]isochromen-10-yl)oxy)ethyl)indolin-2-one (7k)

Yellow solid. ^1H NMR (600 Hz, CDCl_3) 0.74–0.88 (m, 7H), 0.95–0.99 (m, 1H), 1.11–1.16 (m, 1H), 1.31–1.36 (m, 2H), 1.40–1.50 (m, 5H), 1.52–1.57 (m, 1H), 1.78–1.82 (m, 1H), 1.97–2.00 (m, 1H), 2.29 (s, 3H), 2.31–2.34 (m, 1H), 2.52–2.55 (m, 1H), 3.59–3.62 (m, 1H), 3.83–3.87 (m, 1H), 4.06–4.09 (m, 1H), 4.14–4.18 (m, 1H), 4.74 (d, $J = 2.0$ Hz, 1H), 5.13 (s, 1H), 5.25 (s, 2H), 6.80 (d, $J = 4.0$ Hz, 1H), 7.16 (d, $J = 4.0$ Hz, 1H), 7.34–7.47 (m, 5H), 7.75 (s, 1H). ^{13}C NMR (150 Hz, CDCl_3) 163.67, 144.04, 141.67, 136.43, 132.60, 132.40, 128.61, 128.59, 128.42, 128.37, 128.32, 115.79, 108.93, 104.04, 102.22, 87.74, 80.91, 79.30, 64.55, 52.35, 44.18, 39.64, 37.27, 36.36, 34.45, 30.71, 26.12, 24.61, 24.42, 20.99, 20.24, 12.81. HRMS-ESI: m/z Calcd for $\text{C}_{33}\text{H}_{40}\text{N}_2\text{O}_7\text{Na}$ $[\text{M} + \text{Na}]^+$: 599.2728; Found: 599.2715.

3-((Benzyloxy)imino)-6-methyl-1-(3-(((3R,5aS,6R,8aS,9R,12R,12aR)-3,6,9-trimethyldecahydro-12H-3,12-epoxy[1,2]dioxepino[4,3-i]isochromen-10-yl)oxy)propyl)indolin-2-one (7l)

This compound was obtained directly from the collaborators and the detailed synthesis method, together with the characterization data have been reported in Literature [21].

3-((Benzyloxy)imino)-5-methyl-1-(4-(((3R,5aS,6R,8aS,9R,12R,12aR)-3,6,9-trimethyldecahydro-12H-3,12-epoxy[1,2]dioxepino[4,3-i]isochromen-10-yl)oxy)butyl)indolin-2-one (**7m**)

Yellow solid. ¹H NMR (600 Hz, CDCl₃) 0.84–0.98 (m, 7H), 1.22–1.30 (m, 3H), 1.41–1.52 (m, 5H), 1.57–1.77 (m, 6H), 1.85–1.88 (m, 1H), 2.00–2.04 (m, 1H), 2.29 (s, 3H), 2.33–2.38 (m, 1H), 2.59–2.61 (m, 1H), 3.36–3.40 (m, 1H), 3.69–3.88 (m, 3H), 4.76 (d, *J* = 2.0 Hz, 1H), 5.35 (s, 1H), 5.53 (s, 2H), 6.72 (d, *J* = 8.0 Hz, 1H), 7.16 (d, *J* = 8.0 Hz, 1H), 7.35–7.47 (m, 2H), 7.77 (s, 1H). ¹³C NMR (150 Hz, CDCl₃) 163.50, 144.17, 141.65, 136.48, 132.73, 132.40, 128.80, 128.60, 128.40, 128.34, 128.30, 115.95, 108.33, 104.08, 102.05, 87.91, 81.11, 79.26, 67.84, 52.58, 51.69, 44.43, 39.75, 37.42, 36.45, 34.60, 30.91, 27.18, 26.21, 24.66, 24.49, 21.00, 20.36, 13.05. HRMS-ESI: *m/z* Calcd for C₃₅H₄₄N₂O₈Na [M + Na]⁺: 627.3041; Found: 627.3032.

3.2. Pharmacological/Biological Assays

MCF-7, MDA-MB-231, MCF-7/ADR, and MDA-MB-231/ADR breast cancer cell lines (2 × 10³) were plated in each well of a 96-well plate and were allowed to adhere and spread for 24 h. The dihydroartemisinin-5-methylisatin hybrids **6a–e** and **7a–m** were added to a final concentration of 100 μM, and the cells were cultured for 24 h at 37 °C. 3-(4,5-dimethyl-2-thiazolyl)-2,5-diphenyltetrazolium bromide (MTT) solution (10 μL) was added to each well, and the cultures were incubated for an additional 4 h. A further 100 μL of MTT solution was added and incubation continued overnight. The absorbance at 540 nm was determined in each well with a 96-well plate reader. The growth of the treated cells was compared with that of untreated cells.

4. Conclusions

In this study, the influence of the carbon spacers between DHA and isatin moieties in DHA-5-methylisatin hybrids were investigated. The preliminary results illustrated that the length of the carbon spacer was the main parameter affected the activity, and hybrids tethered via the two-carbon linker showed the highest activity. Hydrogen bond donors at C-3 position of isatin moiety could enhance the activity and alkyloxime at C-3 position of isatin moiety could improve the activity to some extent, while benzoxime decreased the activity. The enriched SARs may facilitate further structural modifications.

In particular, the representative hybrid **7a** not only demonstrated profound activity against both drug-sensitive and drug-resistant breast cancer cell lines, but also possessed excellent safety and selectivity profile. Therefore, hybrid **7a** was a promising candidate for the treatment of both drug-sensitive and drug-resistant breast cancers and worthy of further preclinical evaluations.

Supplementary Materials: The following supporting information can be downloaded at: <https://www.mdpi.com/article/10.3390/molecules27227994/s1>, Figures: NMR analysis and MS analysis of the compounds.

Author Contributions: Conceptualization, W.C.; methodology, W.C. and Y.Y.; validation, Y.Y. and H.W.; investigation, Y.Y., H.W.; data curation, Y.Y.; writing—original draft preparation, Y.Y. and J.X.; writing—review and editing, W.C. and F.G.; supervision, F.G. All authors have read and agreed to the published version of the manuscript.

Funding: This research received no external funding.

Institutional Review Board Statement: Not applicable.

Informed Consent Statement: Not applicable.

Data Availability Statement: Not applicable.

Conflicts of Interest: The authors declare no conflict of interest.

Sample Availability: Samples of the compounds are available from the authors.

References

1. Anderson, B.O.; Ilbawi, A.M.; Fidarova, E.; Weiderpass, E.; Stevens, L.; Abdel-Wahab, M.; Mikkelsen, B. The global breast cancer initiative: A strategic collaboration to strengthen health care for non-communicable diseases. *Lancet Oncol.* **2021**, *22*, 578–581. [[CrossRef](#)]
2. Ferlay, J.; Colombet, M.; Soerjomataram, I.; Parkin, D.M.; Piñeros, M.; Znaor, A. Cancer statistics for the year 2020: An overview. *Int. J. Cancer* **2021**, *149*, 778–789. [[CrossRef](#)] [[PubMed](#)]
3. Arnold, M.; Morgan, E.; Runggay, H.; Mafra, A.; Singh, D.; Laversanne, M.; Vignat, J.; Gralow, J.R.; Cardoso, F.; Siesling, S.; et al. Current and future burden of breast cancer: Global statistics for 2020 and 2040. *Breast* **2022**, *66*, 15–23. [[CrossRef](#)] [[PubMed](#)]
4. Sung, H.; Ferlay, J.; Siegel, R.L.; Laversanne, M.; Soerjomataram, I.; Jemal, A.; Bray, F. Global cancer statistics 2020: GLOBOCAN estimates of incidence and mortality worldwide for 36 cancers in 185 countries. *CA Cancer J. Clin.* **2021**, *71*, 209–249. [[CrossRef](#)] [[PubMed](#)]
5. Tufail, M.; Cui, J.; Wu, C. Breast cancer: Molecular mechanisms of underlying resistance and therapeutic approaches. *Am. J. Cancer Res.* **2022**, *12*, 2920–2949. [[PubMed](#)]
6. Li, Y.F.; Li, Z. Potential mechanism underlying the role of mitochondria in breast cancer drug resistance and its related treatment prospects. *Front. Oncol.* **2021**, *11*, e629614. [[CrossRef](#)]
7. Costa, N.S.; Silva, A.S.A.; Melo-Neto, J.S. Effects of dance therapy in women with breast cancer: A systematic review protocol. *PLoS ONE* **2022**, *17*, e0257948.
8. Akram, M.; Iqbal, M.; Daniyal, M.; Khan, A.U. Awareness and current knowledge of breast cancer. *Biol. Res.* **2017**, *50*, e33. [[CrossRef](#)]
9. Li, Q.; Ma, Q.; Cheng, J.; Zhou, X.; Pu, W.; Zhong, X.; Guo, X. Dihydroartemisinin as a sensitizing agent in cancer therapies. *OncoTargets Ther.* **2021**, *14*, 2563–2573. [[CrossRef](#)]
10. Kiani, B.H.; Kayani, W.K.; Khayam, A.U.; Dilshad, E.; Ismail, H.; Mirza, B. Artemisinin and its derivatives: A promising cancer therapy. *Mol. Biol. Rep.* **2020**, *47*, 6321–6336. [[CrossRef](#)]
11. Yu, R.; Jin, C.; Fujimoto, M. Dihydroartemisinin: A potential drug for the treatment of malignancies and inflammatory diseases. *Front. Oncol.* **2021**, *11*, e722331. [[CrossRef](#)] [[PubMed](#)]
12. Dai, X.; Zhang, X.; Chen, W.; Chen, Y.; Zhang, Q.; Mo, S.; Lu, J. Dihydroartemisinin: A potential natural anticancer drug. *Int. J. Biol. Sci.* **2021**, *17*, 603–622. [[CrossRef](#)] [[PubMed](#)]
13. Medvedev, A.; Buneeva, O.; Gnedenko, O.; Ershov, P.; Ivanov, A. Isatin, an endogenous nonpeptide biofactor: A review of its molecular targets, mechanisms of actions, and their biomedical implications. *BioFactors* **2018**, *44*, 95–108. [[CrossRef](#)] [[PubMed](#)]
14. Nath, P.; Mukherjee, A.; Mukherjee, S.; Banerjee, S.; Das, S.; Banerjee, S. Isatin: A scaffold with immense biodiversity. *Mini-Rev. Med. Chem.* **2021**, *21*, 1096–1112. [[CrossRef](#)]
15. Paiva, R.E.F.; Vieira, E.G.; Silva, D.R.; Wegermann, C.A.; Ferreira, A.M.C. Anticancer compounds based on isatin-derivatives: Strategies to ameliorate selectivity and efficiency. *Front. Mol. Biosci.* **2020**, *7*, e627272. [[CrossRef](#)]
16. Sachdeva, H.; Mathur, J.; Guleria, A. Indole derivatives as potential anticancer agents: A review. *J. Chil. Chem. Soc.* **2020**, *65*, 4900–4907. [[CrossRef](#)]
17. Guo, H.; Diao, Q.P. The anti-breast cancer potential of Bis-Isatin scaffolds. *Curr. Top. Med. Chem.* **2020**, *20*, 1499–1503. [[CrossRef](#)]
18. Evdokimov, N.M.; Magedov, I.V.; McBrayer, D.; Kornienko, A. Isatin derivatives with activity against apoptosis-resistant cancer cells. *Bioorganic Med. Chem. Lett.* **2016**, *26*, 1558–1560. [[CrossRef](#)]
19. Wang, Y.; Ding, R.; Tai, Z.; Hou, H.; Gao, F.; Sun, X. Artemisinin-isatin hybrids with potential antiproliferative activity against breast cancer. *Arab. J. Chem.* **2022**, *15*, e103639. [[CrossRef](#)]
20. Hou, H.; Qu, B.; Su, C.; Hou, G.; Gao, F. Design, synthesis and anti-lung cancer evaluation of 1,2,3-Triazole tethered dihydroartemisinin-isatin hybrids. *Front. Pharm.* **2021**, *12*, e801580. [[CrossRef](#)]
21. Zhang, Z.; Zhang, D.; Zhou, Y.; Wang, F.; Xin, A.; Gao, F.; Wang, P.; Zhang, P. The anti-lung cancer activity of propylene tethered dihydroartemisinin-isatin hybrids. *Arab. J. Chem.* **2022**, *15*, e103721. [[CrossRef](#)]
22. Dong, M.; Gao, F.; Li, M.; Zheng, G.; Zhong, C. Three-carbon linked dihydroartemisinin-isatin hybrids: Design, synthesis and their antiproliferative anticancer activity. *Front. Pharm.* **2022**, *13*, e834317. [[CrossRef](#)] [[PubMed](#)]